Spectrochimica Acta Part B: Atomic Spectroscopy 193 (2022) 106438

Contents lists available at ScienceDirect

Spectrochimica Acta Part B: Atomic Spectroscopy

journal homepage: www.elsevier.com/locate/sab

Matrix effect correction method based on the main spectral parameters for rock samples in an *in situ* energy dispersive X-ray fluorescence analysis

Meng Wang [a], Yi Gu [a,b,*], Heng Lu [a], Liangquan Ge [a,b], Qingxian Zhang [a,b], Guoqiang Zeng [a,b]

[a] College of Nuclear Technology and Automation Engineering, Chengdu University of Technology, Chengdu 610059, China
[b] Key Laboratory of Applied Nuclear Techniques in Geosciences Sichuan, Chengdu University of Technology, Chengdu 610059, China

ARTICLE INFO

Keywords:
Monte Carlo simulation
Energy-dispersive X-ray fluorescence analysis
Matrix effect classification
Correction method

ABSTRACT

Due to the differences in the matrix effects between different types of rocks, the target element contents in different rocks cannot be accurately determined by *in situ* X-ray fluorescence (XRF) analyses with the same parameters of the quantification procedure. We investigated the matrix effect correction methods of an *in situ* energy dispersive X-ray fluorescence (EDXRF) analysis for different matrix rock samples using Monte Carlo simulations (17 types of rock samples) and experimental verification (10 types of rock samples), in which both Cu and Zn were selected as target elements. The following conclusions were drawn. The matrix effect classification of the rock samples was not completely controlled by the detectable elemental composition or petrographic classification. According to the correlation between the spectral parameters and the characteristic X-ray intensity of the target elements, the matrix effect classification of rock samples could be more detailed. For rock samples in the same rock classification set and with the same target element content, the target element K_α X-ray intensity could be accurately described by the main spectral parameters, which include the scattering background at an energy interval of 4–19 keV, the Compton peak and the Rayleigh peak. Then, a matrix effect correction method was established, which allowed for the fast measurement of the target element contents of different rock samples by following the same parameters of the quantification procedure in the *in situ* EDXRF analysis. Simultaneously, six types of rock samples containing 3% Zn were selected as the validation set, and the relative errors of the target element content measurements in different rock samples were all less than 6% using the same parameters of the quantification procedure.

1. Introduction

Portable energy dispersive X-ray fluorescence (EDXRF) spectrometry is widely used in the *in situ* elemental composition analysis of rocks and minerals in geological sciences [1–3]. EDXRF has the advantages of convenient operation, rapid *in situ* detection, and non-destructive multielement analysis [4]; however, the matrix effect of the sample is one of the main factors that determines the quality of EDXRF data, and if the effective matrix effect correction is absent, then the reliability of the sample analysis results will be markedly reduced [5,6]. Consequently, matrix effect correction is important to enhance the accuracy of portable EDXRF analyses.

To improve the accuracy of EDXRF analyses, matrix effect calibration curves for different target elements in rock samples have been established, and many matrix effect correction methods, such as the fundamental parameter method [7–9], empirical coefficients method [10], influence coefficient method [11,12] and external standard method [13,14], have been widely used to correct the absorption enhancement effects between elements within the matrix. In geological surveys, the hybrid correction method, which combines the fundamental parameters method and the empirical coefficients method [15], and the external standard method [16] are the main methods used to correct the matrix effect. Due to the complexity of rock-forming conditions and the differences in chemical compositions, the matrices of different rock types have marked differences. Most conventional correction methods are built on samples with similar elemental compositions in close concentration ranges. Thus, the parameters of the quantification procedure for a specific type of rock that is based on conventional correction methods may not be applicable to other types of rocks [17].

In the past, many methods have been successively proposed to address this issue. For example, the correction equations for target elements in different rock types were used to correct the values obtained at

* Corresponding author at: College of Nuclear Technology and Automation Engineering, Chengdu University of Technology, Chengdu 610059, China.
E-mail address: guyi10@cdut.edu.cn (Y. Gu).

https://doi.org/10.1016/j.sab.2022.106438
Received 27 October 2021; Received in revised form 19 April 2022; Accepted 3 May 2022
Available online 7 May 2022

the quantification procedure provided by the instrument manufacturer [3]. The carbonate-specific quantification procedure was proposed based on the method of statistical analyses for the target element content between EDXRF and other conventional methods (*i.e.*, WD-XRF, ICP–MS and ICP–OES), but this quantification procedure could not be used for other rock types, which differ in the elemental concentration ranges and matrix [18]. The internal regression quantification procedure for mudrock based on a reliable elemental dataset from hierarchical cluster analyses can provide qualitative elemental data from uncalibrated measurement instruments [19]. However, due to the effects of the variation in the instrument performance, the quality of the EDXRF data [20], and the limitation of applying these methods to specific rock types, it is difficult to obtain satisfactory results for all rock types with these methods. Recently, some more complex matrix effect correction methods, such as the iterative Monte Carlo method [21], have been implemented in EDXRF analyses. Although those complex matrix effect correction methods could be applied to the matrix effect correction for different rock types, those methods require powerful data processing capabilities, which is the main factor that limits their wide application in *in situ* EDXRF analyses. Therefore, it is necessary to study the difference in the matrix effects between different rock types to establish the matrix effect correction method of *in situ* EDXRF analyses that can quickly and accurately determine the target element contents of different rock samples with the same quantification procedure parameters.

In addition, it is difficult to collect or prepare some measurement materials for EDXRF analyses, and Monte Carlo simulations have long been used as an alternative method for preliminary experimental analysis [22–24]. The advantage of a Monte Carlo simulation is that it can take all physical phenomena that occur during the lifetime of a photon into account [25]. When the measurement conditions of EDXRF analysis and elemental composition of the sample to be tested are known, then the complete spectral response of EDXRF for this sample can be obtained by Monte Carlo simulation.

In this study, we discuss the use of the matrix effect classification of EDXRF for different rock samples through Monte Carlo simulations and develop a matrix effect correction method that can be used to determine the target element contents of different rock samples with the same parameters of the quantification procedure in the *in situ* EDXRF analysis. A confirmatory experiment also demonstrated the effects of the matrix effect classification of different rock samples and the practicality of the matrix effect correction method.

2. Matrix effect classification of Cu by Monte Carlo simulation

2.1. Simulation parameters

Because a large variety of rock samples are required for matrix effect analyses, and some samples are difficult to collect or prepare, a Monte Carlo simulation is initially chosen to investigate matrix effects in an EDXRF analysis. Portable EDXRF spectra simulations are performed with the open-source software Geant4, which is a general-purpose Monte Carlo toolkit that can be used to describe particle interactions in matter in the energy range from a few eV to TeV [26]. In Monte Carlo simulation, only the geometric setup of the portable EDXRF spectrometer and the elemental composition of the sample must be set to obtain the EDXRF simulation spectra of the corresponding samples. The geometric setup references the structure of the conventional portable EDXRF spectrometer and the technical data sheet of a miniature X-ray tube by Moxtek, Inc. [27] The miniature X-ray tube was provided with a collimator that has a 2-mm-diameter hole, a silver (Ag) transmission target, and a 250-μm-thick beryllium end window. Electrons with a 35-kV accelerating voltage bombard the 2-μm-thick Ag target within a diameter range of 1.6 mm; these electrons are then used to induce X-ray emission, where the X-ray emission angle is 46°. The vertical distance between the X-ray exit portal and the top surface of the rock sample is 7 mm, and the angle between the detector axis and the X-ray emission axis is 80°. The geometric setup of the portable EDXRF setup is shown in Fig. S1 (Appendix) in the supplementary material. The purpose of using Monte Carlo simulations is to obtain the variation pattern of matrix effects for different rock types when the same target element content is measured. To remove the influence of the detector on the simulation results due to the difference in the detection efficiency of different energy rays, the flux-recording module replaces the detector in the model of Fig. S1 (Appendix). For the difference between the simulation spectra obtained using the detector and the flux-recording module, there is a difference in the detection efficiency of the former for different energy rays, while the latter is the same. Due to this difference, the spectral intensity of the simulation spectra cannot compare directly with the measured spectra, but the variation pattern of matrix effects for different rock types can be obtained completely, and this variation pattern is applicable to EDXRF spectrometers equipped with different types of detectors.

There were 17 types of metallogenetic rock samples used in the Monte Carlo simulations to obtain the EDXRF spectra; these types of samples included 13 types of igneous rocks (granite, pantellerite, diorite, quartz diorite, monzodiorite, andesite, syenite, monzonite, quartz monzonite, gabbro, anorthosite, biotite carbonatite, and calcite carbonatite), 2 types of metamorphic rocks (phyllite and mica schist), and 2 types of sedimentary rocks (limestone and dolomitic limestone). The elemental compositions of the rock samples were consistent with relevant geological data and the GeoReM Database [28]. The elemental composition data for all the rock samples are listed in Table S1 (Appendix) in the supplementary material. In addition, each rock sample contained the same Cu contents of 2%, 3%, 4%, and 5% by weight. Each rock sample had the same simulation parameters, such as moisture and density, except for the elemental compositions. Thus, the variation in the Cu K_α X-ray intensity of the EDXRF spectra was entirely caused by the matrix effect of the rock samples. The portable EDXRF spectra of 17 types of rock samples were simulated, and the simulation spectra of the four rock samples are shown in Fig. 1.

2.2. Matrix effect classification of the different rock types

The similarity of the elemental composition of the rock samples was studied using cluster analysis, which was the main method used for rock source analysis, and different rock samples could be classified by this method according to the degree of elemental composition similarity. The results of the cluster analysis of the elemental compositions of all the rock samples are shown in Fig. S2 (Appendix). Biotite carbonate, calcite carbonate, limestone, and dolomitic limestone have many similarities in terms of elemental composition, while the elemental compositions of the other 13 types of rock samples are also similar.

The main spectral parameters that have the closest relationship with the variation in the Cu K_α X-ray intensity according to the matrix effect for all rock types were extracted by correlation analysis. The EDXRF spectra of each rock type with the same Cu content (2% by weight) were simulated, and the results of the correlation analysis of those spectral parameters are listed in Table S2 (Appendix). The correlation scatter diagrams between the Cu K_α X-ray and some spectral parameters are also shown in Fig. S3 (Appendix). The intensity of the Cu K_α X-ray exhibited a strong linear correlation with the intensity of the spectral parameters, including the scattering background at the energy interval of 4–19 keV, the Compton peak and the Rayleigh peak of all the rock types except for biotite carbonate and calcite carbonate. Because the Compton and Rayleigh peaks are similarly affected by the matrix effect, they can retain a strong linear correlation with the intensity of Cu K_α X-rays in different rock types. The scattering background also has a strong linear correlation with the intensity of the Cu K_α X-ray due to its more sensitive reflection to the change in the sample matrix, which is consistent with the conclusions of Bastos et al. [29] For the K-series X-ray intensity of Si and K, those spectral parameters have a weak linear correlation with the Cu K_α X-ray intensity due to absorption-enhancement effects caused by

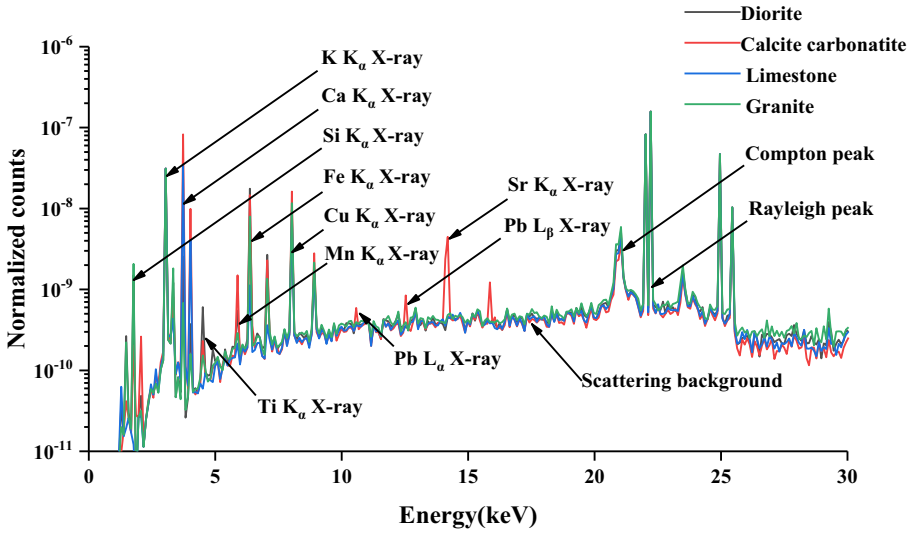

Fig. 1. EDXRF simulation spectra of four kinds of rock samples with 2% Cu by weight.

other elements in the rocks, such as Ca and Fe. The Ca, Ti, Mn, and Fe contents varied markedly depending on the lithology of the rock samples; thus, their linear correlations with the Cu K_α X-ray intensity were not considered.

Based on the results of the correlation analysis between the Cu K_α X-ray intensity and those spectral parameters, two igneous rocks (biotite carbonate and calcite carbonate) differed from the other 15 types of rock including limestone and dolomite limestone, where those 15 types of rock belong to the same classification set under the correlation analysis. Comparing the two igneous rocks (biotite carbonate and calcite carbonate) with the two sedimentary rocks (limestone and dolomite limestone), the variation in the Cu K_α X-ray intensity caused by the matrix effect was markedly different. Thus, it is insufficient to consider the matrix effect classification of the target element in the rock samples simply based on petrographic classification or detectable elemental composition similarity. This classification should include a correlation analysis of the spectral parameters and the target element K_α X-ray intensity in the EDXRF spectra of each rock type.

2.3. Matrix effect correction for the different rock types

According to the results of the correlation analysis of the spectral parameters for the different rock types, the main spectral parameters, which had a strong linear correlation with the intensity of the target element K_α X-rays, were used to correct the matrix effects between different rock types in the same rock classification set. In the *in situ* EDXRF analysis, low-energy X-rays, such as the K_α X-rays of Si and K, are more severely affected by air absorption than X-rays with other energies. Additionally, the enhancement effects of other elements in the rock samples are also strong for the K_α X-ray intensities of Si and K. Therefore, the main spectral parameters that were less affected by the measurement conditions and that had a strong linear correlation with the intensity of the target element K_α X-rays in the *in situ* EDXRF analysis were selected for the matrix effect correction. Then, the target element K_α X-ray intensity was described by the main spectral parameters, which included the scattering background at an energy interval of 4–19 keV, the Compton peak, and the Rayleigh peak through the following equation:

$$N_x = A + k_1 \cdot N_{BG} + k_2 \cdot N_R + k_3 \cdot N_C \quad (1)$$

where N_x is the intensity of the target element K_α X-rays; N_{BG} is the intensity of the scattering background at the energy interval of 4–19 keV; N_R is the intensity of the Rayleigh peak; N_C is the intensity of the Compton peak; k_1, k_2, and k_3 are the least-squares fitting coefficients for the main spectral parameters; and A is the constant term.

Eq. (1) shows that the intensity of target element K_α X-rays of the different rock types in the same rock classification set and with the same target element content could be described by those main spectral parameters. The constant term and the fitting coefficients k_1, k_2, and k_3 for Eq. (1) were fixed with the same target element contents for the different rock types. When the target element is Cu, the relative errors between the Cu K_α X-ray counts obtained by simulation and those obtained by fitting for each rock type with a 2% Cu content are listed in Table 1. Except for the biotite carbonate and calcite carbonate rock samples, the values of the relative errors were all below 2%.

The main spectral parameters of the EDXRF simulation spectra for each rock type with different Cu contents were fitted by least squares to derive the constant terms and the fitting coefficients k_1, k_2, and k_3 in Eq. (1), where the fitting results for the different Cu contents are listed in Table S3 (Appendix). Because the degrees of the effects of those main spectral parameters on the target element K_α X-ray intensity mainly depended on the EDXRF measurement instrument, the measurement

Table 1
Relative errors of the Cu K_α X-ray intensity fitting by the scattering background intensity, Compton peak, and Rayleigh peak.

Rock type	Cu Kα X-ray counts by simulation ($\times 10^{-9}$)	Cu Kα X-ray counts by fitting ($\times 10^{-9}$)	Relative errors (%)
Andesite	9.80	9.72	−0.76
Dolomitic limestone	8.29	8.23	−0.73
Monzodiorite	10.19	10.28	0.92
Monzonite	10.54	10.46	−0.79
Gabbro	7.31	7.38	0.93
Granite	11.64	11.70	0.47
Pantellerite	10.58	10.53	−0.45
Phyllite	9.87	9.76	−1.14
Diorite	9.59	9.67	0.83
Limestone	8.23	8.23	−0.06
Quartz monzonite	11.25	11.23	−0.15
Quartzdiorite	9.54	9.61	0.75
Gabbro	10.68	10.89	1.90
Mica schist	10.04	10.01	−0.41
Syenite	11.39	11.27	−1.02
Calcite carbonatite	5.02	6.85	36.40
Biotite carbonatite	4.52	6.93	53.21

parameters, and the target element species, the fitting coefficients k_1, k_2, and k_3 in Table S3 (Appendix) essentially remained constant with the different Cu contents. The scatter diagram of the constant term (*A*) of Eq. (1) with the Cu content is shown in Fig. 2. The constant term had a high linear correlation with the Cu content; therefore, the Cu content for the rock sample could be determined by the constant term.

In practical applications, based on matrix effect classification *via* correlation analysis between the main spectral parameters and the target element K_α X-ray intensity, the specific steps of this matrix effect correction method for different rock types in the same rock classification set are listed as follows:

(1) Acquisition of quantitative parameters
   a. Based on physical experiments, the EDXRF spectra of different rock types with the same target element contents are obtained, and then based on the least-squares fitting between the intensity of the main spectral parameters and the K_α X-ray intensity of the target element, the constant terms (*A*) and the fitting coefficients k_1, k_2, and k_3 in Eq. (1) can be determined. The fitting coefficients k_1, k_2 and k_3 remain constant with the different target element contents.
   b. Any rock type in the same rock classification set is selected as the standard rock sample. Based on the EDXRF spectra of the standard rock samples with different target element contents, the constant term (*A*) in Eq. (1) under different target element contents is calculated by the fitting coefficients k_1, k_2, and k_3 and the K_α X-ray intensity of the target element at different contents. Then, the fitting formula of the target element content and the constant term (*A*) in Eq. (1) is established. Finally, all rock samples in the same rock classification set can be quantitatively analysed using the fitting formula for the target element content and the fitting coefficients k_1, k_2 and k_3. For other rock classification sets, the fitting formula and the fitting coefficients must be recalculated.
(2) Quantitative analysis of the target elements in rock samples

For any rock sample to be tested quantitatively, it is necessary to select the quantitative procedure of the corresponding rock classification set, which is based on the lithology of the test rock sample, and the target element content is determined:

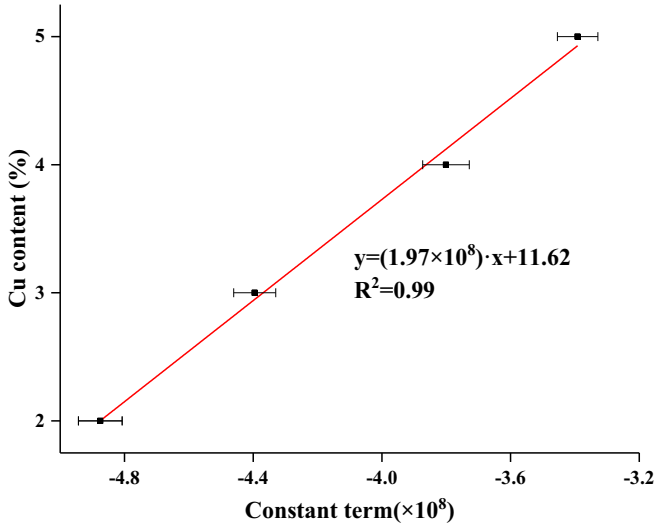

Fig. 2. Scatter diagram between the Cu content and the constant term; the red line shows the fitting curve for the linear relationship. (Error bars are the fitted standard error of the constant term under different Cu contents). (For interpretation of the references to colour in this figure legend, the reader is referred to the web version of this article.)

   a. Based on the intensity of the main spectral parameters and the K_α X-ray intensity of the target element in the EDXRF spectra for the test rock sample, the constant term (*A*) can be calculated with Eq. (1).
   b. According to the fitting formula between the target element content and the constant term (*A*), the target element content in the test rock sample can be calculated.

3. Experimental verification

Ten rock masses (griotte, syenite, fine-grained granite, medium-grained granite, fine-grained mica schist, coarse-grained mica schist, andesite, coarse-grained gabbro, limestone, and calcite carbonate) were collected and used for the confirmatory experiment. The EDXRF spectra of these rock samples were measured using a portable EDXRF spectrometer with an Ag target (35 kV, 2 μA) developed by the Chengdu University of Technology. This instrument had limits of detection of <5 mg/kg and < 4 mg/kg for Cu and Zn, respectively after a measurement time of 300 s. The contents of both Zn and Cu in those rock samples were below the limit of detection. To demonstrate the feasibility and practicality of the matrix effect classification in this study, these two elements were selected as target elements to test the effects of matrix effect classification. The compounds added to rock samples for Cu and Zn were highly purified Cu powder and ZnO, respectively. In addition, the matrix effect correction method in this study was established based on the simulated spectra of different rock samples with Cu as the target element. Therefore, Zn was only selected as the target element to demonstrate whether this method has a higher universality for a target element other than Cu.

In the experiment to confirm the efficiency of matrix effect classification, all the rock masses were powdered by hand using an agate mortar and pestle, a mass fraction of a 2% target element was uniformly added to prepare samples with the same target element, and all rock samples were edged with boric acid. According to previous studies, the rock samples were measured using a portable EDXRF spectrometer after a measurement time of 300 s [30,31], and the EDXRF spectra values for all the rock samples were determined by averaging triplicate measurements. The RSD (relative standard deviation) for the target elements (2% Cu and 2% Zn) K_α X-ray count rate over 300 s was less than 2.6% for 30 consecutive measurements of the same sample with this EDXRF measurement instrument. The measured spectra for some rock samples with a Cu content of 2% by weight are shown in Fig. 3.

According to the measured spectra of those rock samples, the results of the correlation analysis between the Cu K_α X-ray intensity and the main spectral parameters are shown in Fig. 4. The target element K_α X-ray intensities of Zn and Cu had good linear correlations with the intensity of the scattering background at an energy interval of 4–19 keV, the Compton peak, and the Rayleigh peak. However, this result was not observed for the calcite carbonate rock sample, and the variation in the target element K_α X-ray intensity of calcite carbonate caused by the matrix effect was markedly different from that of the other nine rock samples due to the much higher concentrations of Ca, Mg, Sr and other elements in calcite carbonate [32]. The target element K_α X-ray intensity had a weak linear correlation with the Si and K K_α X-ray intensities due to the absorption of low-energy X-rays by air in the experiment. This result is consistent with the analysis of the relationship of the simulated spectra.

Based on Eq. (1) and the EDXRF measurement spectra of the different rock samples, the constant term (*A*) and the fitting coefficients k_1, k_2, and k_3 for different rock samples with 2% target element contents were obtained by least-squares fitting and are listed in Table S4 (Appendix). The relative errors between the target element K_α X-ray counts obtained by measurement and those obtained by fitting are listed in Table 2. Except for the calcite carbonate rock sample, the relative errors for the target element of Cu are less than 3.45%, and the relative errors of Zn are less than 6.22%.

In the confirmatory experiment for the matrix effect correction, six

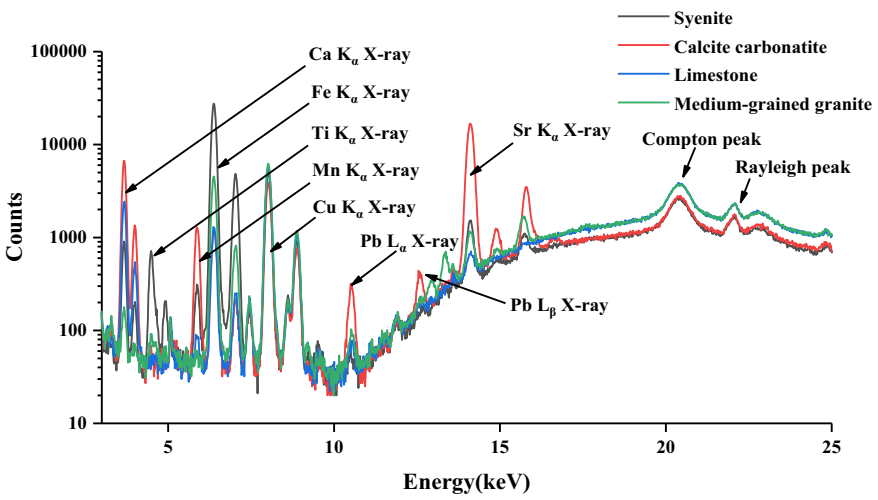

Fig. 3. EDXRF measured spectra of four kinds of rock samples with 2% Cu by weight. (Spectra data are the average of 3 repeated measurements).

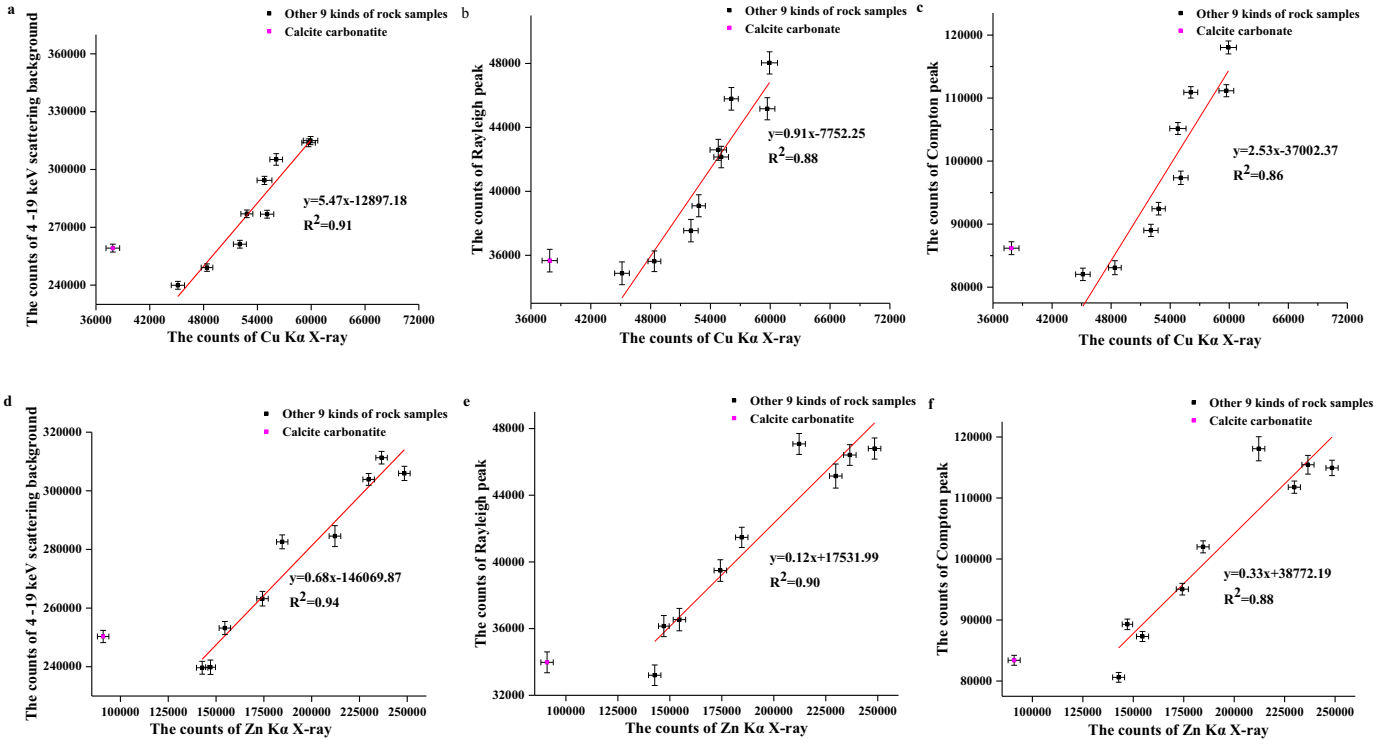

Fig. 4. Correlation scatter diagram of the target elements K_α X-ray intensities and the main spectra parameters. (Data and error bars are the average and standard deviation of 3 repetitions for the target elements K_α X-ray intensities and the main spectra parameters).

types of rock samples with a 3% Zn content were prepared as the validation set using the same method, and the EDXRF spectra of those rock samples were measured by the same EDXRF measurement instrument and measurement parameters. The compound of Zn added in those rock samples is also ZnO. Then, coarse-grained gabbro rock samples that contained 1, 2, 3, and 4% Zn contents were selected as the standard rock samples, and the standard rock samples were also prepared using the same method. Then, the standard rock samples were used to obtain the fitting formula of the target element content and the constant term (*A*).

According to the fitting coefficients k_1, k_2, and k_3 remaining constant with different target element contents, the fitting coefficients k_1, k_2, and k_3 for Eq. (1) with the target element Zn at different contents were the same as in Table 2 for a 2% Zn content. Based on the measured spectra of the coarse-grained gabbro samples with different Zn contents, the constant term (*A*) in Eq. (1) with different Zn contents was calculated, and the fitting formula of the Zn content and the constant term is shown in Fig. 5.

The corrected Zn content of the test rock samples was calculated with the fitting formula in Fig. 5, and the corrected Zn content in all the test rock samples is listed in Table 3. The uncorrected Zn contents are also shown in Table 3, which were obtained by the Zn K_α X-ray count quantitative curves of the standard rock samples. The relative errors between the corrected Zn content and the true content of the test rock samples were less than 6%, except for that of calcite carbonate. The relative errors of the corrected Zn contents thus were much lower than those of the uncorrected Zn contents.

According to the results of the confirmatory experiment with different target elements, this classification of matrix effects can be

Table 2
Relative errors of the target element K_α X-ray intensity fitting by scattering background, Compton peak, and Rayleigh peak with 2% target element.

Rock type	Cu			Zn		
	Measured value*	Fitted value*	Relative error (%)	Measured value	Fitted value	Relative error (%)
Andesite	56,095	58,030	3.45	229,805	226,223	−1.56
Coarse grain gabbro	48,380	48,363	−0.04	134,590	138,803	3.13
Coarse grain mica schist	55,082	54,556	−0.96	162,296	161,609	−0.42
Griotte	54,790	54,963	0.32	192,179	193,078	0.47
Limestone	45,133	46,043	2.02	97,100	96,629	−0.48
Fine-grained granite	59,710	59,096	−1.03	236,562	238,412	0.78
Fine-grained mica schist	52,826	53,645	1.55	173,974	184,803	6.22
Syenite	52,046	50,191	−3.56	101,442	95,156	−6.20
Medium-grained granite	59,925	59,109	−1.36	248,485	241,713	−2.73
Calcite carbonatite	37,880	49,062	29.52	90,951	108,289	19.06

* The measured value and the fitted value are the target element K_α X-ray counts at a measurement time of 300 s.

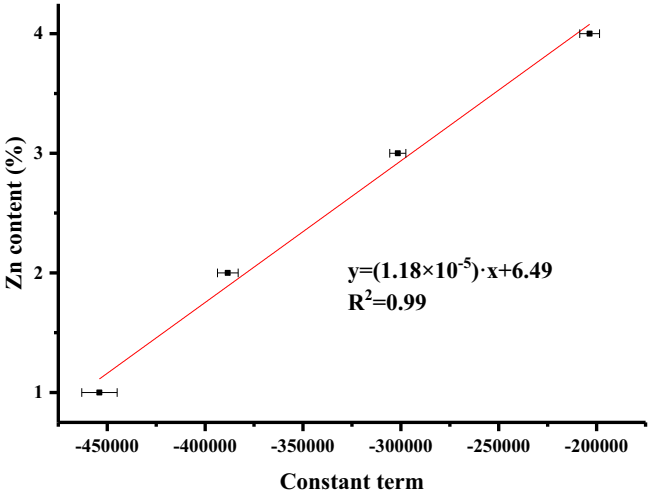

Fig. 5. Scatter diagram of the Zn content and the constant term. The red line shows the fitting curve for the linear relationship. (Error bars are the fitted standard error of the constant term under different Cu contents). (For interpretation of the references to colour in this figure legend, the reader is referred to the web version of this article.)

applied to different target elements, and the target element K_α X-ray intensity can be described by the intensity of the scattering background at the energy interval of 4–19 keV, the Compton peak, and the Rayleigh peak for different rock samples in the same rock classification set.

For the confirmation experiments of the test samples, the matrix effect correction method in this study can be applied to the target element quantification analysis of different rock samples, and the relative error of the measurement results of those test rock samples under the target element of Zn are all less than 6%.

4. Discussion

For the matrix effect correction method developed in this study, the expected analysed objects are mainly mineralized rock samples, and this method can be applied to rock samples with target element contents in the range of 10^3-10^5mg/kg. For the rock samples with low target element contents, the applicability of this method must be systematically studied.

Although the matrix effects of the different target elements in some types of rock samples analysed by *in situ* EDXRF were studied, the lithologic categories and the target elements were not comprehensive, and whether the L-series X-ray intensity of heavy atomic number elements can be described by the main spectral parameters must be systematically studied in more detail.

5. Conclusion

According to Monte Carlo simulations and experimental verification, we analysed the difference in matrix effects for different matrix rock samples, and the following conclusions were drawn:

(1) To classify the matrix effect, the effects of the matrix of different rock samples on the results of the target element analysis are not completely controlled by petrographic classification or the detectable elemental composition in EDXRF. The matrix effect classification of rock samples can be more delicate through a correlation analysis of the main spectral parameters and the characteristic X-ray intensity of the target element in the EDXRF spectra.
(2) For different rock samples in the same rock classification set, the target element K_α X-ray intensity can be accurately described by the intensity of the scattering background, the Compton peak, and the Rayleigh peak. Based on the results of measuring the test rock samples under the target element of 3% Zn, the target element contents of the test rock samples can be accurately determined through the matrix effect correction method used in this study, and this method provides the possibility of quickly determining the target element contents in different rock samples under the same parameters of the quantification procedure in an *in situ* EDXRF analysis. This study also provides a new idea for studying matrix effect correction in an *in situ* EDXRF analysis.
(3) This matrix effect correction method in this study is not limited to a specific type of rock but requires a similar matrix effect in different rocks. In practical applications, when a sufficient

Table 3
Relative error between the Zn contents obtained by measurement and the true values of the test rock samples with a 3% Zn content.

Rock type	True contten (%)	Corrected Zn content (%)	Relative errors (%)	Uncorrected Zn content (%)	Relative errors (%)
Andesite	3.00	2.92 ± 0.02	−2.71	3.56 ± 0.04	18.53
Coarse grain mica schist	3.00	3.03 ± 0.05	0.90	2.72 ± 0.03	−9.25
Griotte	3.00	2.94 ± 0.03	−1.96	3.26 ± 0.01	8.81
Limestone	3.00	2.83 ± 0.01	−5.53	2.27 ± 0.02	−24.33
Fine-grained granite	3.00	2.97 ± 0.04	−1.15	3.56 ± 0.02	18.74
Calcite carbonatite	3.00	2.23 ± 0.03	−25.67	2.10 ± 0.05	−30.13

number of quantitative procedures corresponding to different rock classification sets are prepared in advance, it is only necessary to select the quantitative procedure of the corresponding rock classification set according to the lithology of the rock sample to achieve a quantitative analysis of the rock sample.

CRediT authorship contribution statement

Meng Wang: Conceptualization, Methodology, Writing – review & editing. **Yi Gu:** Conceptualization, Methodology, Writing – review & editing. **Heng Lu:** Conceptualization, Writing – review & editing. **Liangquan Ge:** Methodology. **Qingxian Zhang:** Methodology. **Guoqiang Zeng:** Methodology.

Declaration of Competing Interest

The authors declare that they have no known competing financial interests or personal relationships that could have appeared to influence the work reported in this paper.

Acknowledgments

The authors acknowledge the financial support by the National Key R&D Program of China (Project No. 2017YFC0602100), the National Science Foundation of China (Project No. 42127807), and Sichuan Science and Technology Program (Project No. 2020JDRC0108).

Appendix A. Supplementary data

Supplementary data to this article can be found online at https://doi.org/10.1016/j.sab.2022.106438.

References

[1] Z. Yuan, Q. Cheng, Q. Xia, L. Yao, Z. Chen, R. Zuo, et al., Spatial patterns of geochemical elements measured on rock surfaces by portable X-ray fluorescence: application to hand specimens and rock outcrops, Geochem. Explor. Environ. Analys. 14 (2014) 265–276, https://doi.org/10.1144/geochem2012-173.
[2] D.C. Arne, R.A. Mackie, S.A. Jones, The use of property-scale portable X-ray fluorescence data in gold exploration: advantages and limitations, Geochem. Explor. Environ. Analys. 14 (2014) 233–244, https://doi.org/10.1144/geochem2013-233.
[3] J. Quye-Sawyer, V. Vandeginste, K.J. Johnston, Application of handheld energy-dispersive X-ray fluorescence spectrometry to carbonate studies: opportunities and challenges, J. Anal. Atom. Spectrom. 30 (2015) 1490–1499, https://doi.org/10.1039/C5JA00114E.
[4] E. Frahm, Validity of "off-the-shelf" handheld portable XRF for sourcing near eastern obsidian chip debris, J. Archaeol. Sci. 40 (2013) 1080–1092, https://doi.org/10.1016/j.jas.2012.06.038.
[5] T. Shiraiwa, N. Fujino, Theoretical calculation of fluorescent X-ray intensities in fluorescent X-ray Spectrochemical analysis, Jpn. J. Appl. Phys. 5 (1966) 886–899, https://doi.org/10.1143/jjap.5.886.
[6] M.S. Shackley, X-Ray Fluorescence Spectrometry (XRF) in Geoarchaeology, Springer, New York, 2010.
[7] B. Holyńska, J. Ptasiński, D. Wegrzynek, Software for fundamental parameter method in energy dispersive x-ray fluorescence analysis of intermediate thickness samples, Appl. Radiat. Isot. 45 (1994) 409–414, https://doi.org/10.1016/0969-8043(94)90103-1.
[8] A.A. Shaltout, M.A. Moharram, N.Y. Mostafa, Wavelength dispersive X-ray fluorescence analysis using fundamental parameter approach of *Catha edulis* and other related plant samples, Spectrochim. Acta B At. Spectrosc. 67 (2012) 74–78, https://doi.org/10.1016/j.sab.2012.01.004.
[9] D.K.G. de Boer, Fundamental parameters for X-ray fluorescence analysis, Spectrochim. Acta B At. Spectrosc. 44 (1989) 1171–1190, https://doi.org/10.1016/0584-8547(89)80114-4.
[10] S.D. Rasberry, K.F.J. Heinrich, Calibration for interelement effects in x-ray fluorescence analysis, Anal. Chem. 46 (1974) 81–89, https://doi.org/10.1021/ac60337a027.
[11] G.R. Lachance, Correction procedures using influence coefficients in X-ray fluorescence spectrometry, Spectrochim. Acta B At. Spectrosc. 48 (1993) 343–357, https://doi.org/10.1016/0584-8547(93)80040-2.
[12] A.E. Steiner, R.M. Conrey, J.A. Wolff, PXRF calibrations for volcanic rocks and the application of in-field analysis to the geosciences, Chem. Geol. 453 (2017) 35–54, https://doi.org/10.1016/j.chemgeo.2017.01.023.
[13] R. Sitko, B. Zawisza, Quantification in X-ray fluorescence spectrometry, InTech (2012) 137–162.
[14] P.M.S. Carvalho, S. Pessanha, J. Machado, A.L. Silva, J. Veloso, D. Casal, et al., Energy dispersive X-ray fluorescence quantitative analysis of biological samples with the external standard method, Spectrochim. Acta B At. Spectrosc. 174 (2020), 105991, https://doi.org/10.1016/j.sab.2020.105991.
[15] L. Ge, F. Li, Review of in situ X-ray fluorescence analysis technology in China, X-Ray Spectrom. 49 (2020) 458–470, https://doi.org/10.1002/xrs.3135.
[16] M.S. Shackley, An introduction to X-ray fluorescence (XRF) analysis in archaeology, in: M.S. Shackley (Ed.), X-Ray Fluorescence Spectrometry (XRF) in Geoarchaeology, Springer, New York, New York, NY, 2011, pp. 7–44.
[17] N. Craigie, Application of chemostratigraphy in clastic, carbonate and unconventional reservoirs, in: N. Craigie (Ed.), Principles of Elemental Chemostratigraphy: A Practical User Guide, Springer International Publishing, Cham, 2018, pp. 131–177.
[18] M. Al-Musawi, S. Kaczmarek, A new carbonate-specific quantification procedure for determining elemental concentrations from portable energy-dispersive X-ray fluorescence (PXRF) data, Appl. Geochem. 113 (2020), 104491, https://doi.org/10.1016/j.apgeochem.2019.104491.
[19] K.G. Martin, T.R. Carr, Developing a quantitative mudrock calibration for a handheld energy dispersive X-ray fluorescence spectrometer, Sediment. Geol. 398 (2020), 105584, https://doi.org/10.1016/j.sedgeo.2019.105584.
[20] N.W. Brand, C.J. Brand, Performance comparison of portable XRF instruments, Geochem. Explor. Environ. Analys. 14 (2014) 125–138, https://doi.org/10.1144/geochem2012-172.
[21] T. Trojek, Iterative Monte Carlo procedure for quantitative X-ray fluorescence analysis of copper alloys with a covering layer, Radiat. Phys. Chem. 167 (2020), 108294, https://doi.org/10.1016/j.radphyschem.2019.04.044.
[22] W. Kim, J. Jang, D.H. Kim, Monte Carlo simulation for the analysis of various solid samples using handheld X-ray fluorescence spectrometer and evaluation of the effect by environmental interferences, Spectrochim. Acta B At. Spectrosc. 180 (2021), 106203, https://doi.org/10.1016/j.sab.2021.106203.
[23] F. Burille, J.J.M. Correa, P. Zambianchi, J.K. Zambianchi, M. Antoniassi, Detection of radium in water by x-ray fluorescence using Monte Carlo simulations, Radiat. Phys. Chem. 167 (2020), 108374, https://doi.org/10.1016/j.radphyschem.2019.108374.
[24] T. Trojek, T. Čechák, L. Musílek, Monte Carlo simulations of disturbing effects in quantitative in-situ X-ray fluorescence analysis and microanalysis, Nucl. Instrum. Methods Phys. Res. Sect. A: Acceler. Spectr. Detect. Assoc. Equipm. 619 (2010) 266–269, https://doi.org/10.1016/j.nima.2009.11.079.
[25] T. Schoonjans, L. Vincze, A.S. Vicente, M.S.D.R. Brondeel, G. Silversmit, K. Appel, et al., A general Monte Carlo simulation of energy dispersive X-ray fluorescence spectrometers — part 5: polarized radiation, stratified samples, cascade effects, M-lines, Spectrochim. Acta B At. Spectrosc. 70 (2012) 10–23, https://doi.org/10.1016/j.sab.2012.03.011.
[26] S. Agostinelli, J. Allison, K. Amako, J. Apostolakis, H. Araujo, P. Arce, et al., Geant4—a simulation toolkit, Nucl. Instrum. Methods Phys. Res. Sect. A: Acceler. Spectr. Detect. Assoc. Equipm. 506 (2003) 250–303, https://doi.org/10.1016/S0168-9002(03)01368-8.
[27] G. A, Miniature X-ray sources, J. Microelectromech. S. 26 (2017) 295–302, https://doi.org/10.1109/JMEMS.2016.2640344.
[28] K.P. Jochum, U. Nohl, K. Herwig, E. Lammel, B. Stoll, A.W. Hofmann, GeoReM: a new geochemical database for reference materials and isotopic standards, Geostand. Geoanal. Res. 29 (2005) 333–338, https://doi.org/10.1111/j.1751-908X.2005.tb00904.x.
[29] R.O. Bastos, F.L. Melquiades, G.E.V. Biasi, Correction for the effect of soil moisture on in situ XRF analysis using low-energy background, X-Ray Spectrom. 41 (2012) 304–307, https://doi.org/10.1002/xrs.2397.
[30] G.E.M. Hall, G.F. Bonham-Carter, A. Buchar, Evaluation of portable X-ray fluorescence (pXRF) in exploration and mining: phase 1, control reference materials, Geochem. Explor. Environ. Analys. 14 (2014) 99–123, https://doi.org/10.1144/geochem2013-241.
[31] P.S. Ross, A. Bourke, B. Fresia, Improving lithological discrimination in exploration drill-cores using portable X-ray fluorescence measurements: (1) testing three Olympus Innov-X analysers on unprepared cores, Geochem. Explor. Environ. Analys. 14 (2014) 171–185, https://doi.org/10.1144/geochem2012-163.
[32] N.W. Craigie, Principles of Elemental Chemostratigraphy, Springer, Cham, 2018.